

# END-OF-MISSION PLANNING CHALLENGES FOR A SATELLITE IN A CONSTELLATION

**Ronald J. Boain**

*Jet Propulsion Laboratory/California Institute of Technology*

*4800 Oak Grove Drive*

*Pasadena, California 91109*

*United State of America*

*E-Mail: Ronald.J.Boain@jpl.nasa.gov*

At the end of a mission, satellites embedded in a constellation must first perform propulsive maneuvers to safely exit the constellation before they can begin with the usual end-of-mission activities: deorbit, passivation, and decommissioning. The target orbit for these exit maneuvers must be sufficiently below the remaining constellation satellites such that, once achieved, there is no longer risk of close conjunctions. Yet, the exit maneuvers must be done based on the spacecraft's state of health and operational capability when the decision to end the mission is made. This paper focuses on the recently developed exit strategy for the CloudSat mission to highlight problems and issues, which forced the discarding of CloudSat's original EoM Plan and its replacement with a new plan consistent with changes to the spacecraft's original operational mode. The analyses behind and decisions made in formulating this new exit strategy will be of interest to other missions in a constellation currently preparing to update their End-of-Mission Plan.

## 1. INTRODUCTION

From the moment of a space mission's launch, time is marching toward an inevitable event: the end-of-mission (EoM). The EoM is when the satellite's productive time on orbit is over and it must cease its data collection. In most cases, the spacecraft must also perform deorbit maneuvers to achieve a new perigee low enough that atmospheric entry will occur in 25 years, or less. In addition, after the deorbit maneuvers, the satellite must then systematically passivate and decommission all operating subsystems to place them in their lowest possible internal energy state. Once these activities are completed, the satellite effectively becomes a piece of space debris and the mission is truly ended.

For a satellite embedded in a constellation, the EoM process poses an additional, critical step. The satellite must first exit the constellation without making a close conjunction (or even worse, a collision) with any of the remaining constellation satellites before it can begin taking the final steps of lowering the orbit and ultimately decommissioning the spacecraft.

The Afternoon Constellation (a.k.a. "A-Train") is a prime example of a constellation with several of its satellites operating beyond the limits of their design life. As a result, the A-Train Mission Operations Working

Group (MOWG) has recently recognized this fact and has begun to actively address the EoM and safe constellation exit problem. The MOWG is seeking to understand better what are the strong points and weak points for the constellation exit options.

The A-Train comprises five satellites, from front to back. These are Global Change Observation Mission 1<sup>st</sup>-Water (GCOM W1), Aqua, Cloud-Aerosol Lidar and Infrared Pathfinder Satellite Observations (CALIPSO), CloudSat, and Aura (See Fig. 1). Aqua, CloudSat, and Aura were built and launched by NASA; CALIPSO was provided by CNES and NASA in a cooperative effort; and GCOM W1, launched in May 2012, was provided by JAXA. Planned for a summer 2014 launch, another NASA satellite, Orbiting Carbon Observatory-2 (OCO-2), will take up a position in front of GCOM W1 in the constellation.

For the foreseeable future, the Aqua satellite will remain the anchor of the A-Train. This is because the along-track positions of all the other satellites are measured, in effect, relative to Aqua. Aqua was launched in 2002 with a nominal design life of five years. The other missions—Aura, CALIPSO, CloudSat, and GCOM W1—were launched in the years to follow. Except for GCOM W1, all satellites are operating beyond their target lifetime at launch.

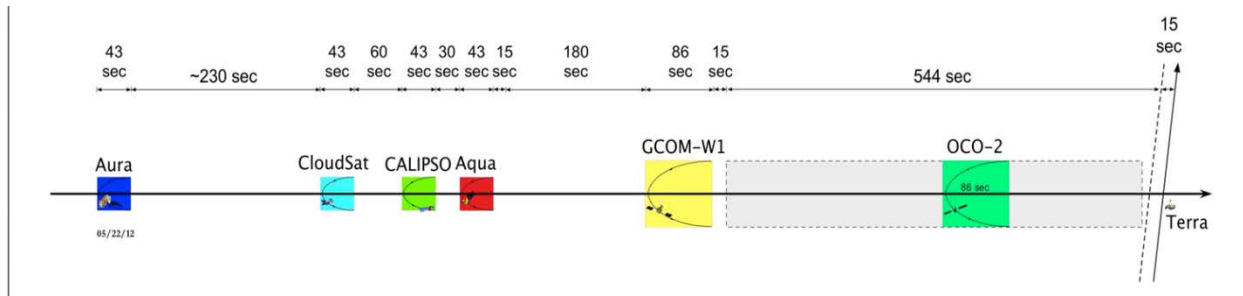


Figure 1. A-Train Constellation Configuration

CALIPSO was launched concurrently with CloudSat on a shared launch in April 2006 and has been operating in the A-Train ever since. Its remaining propellant will likely limit its lifetime as a participating member of the A-Train. In March 2013, the CALIPSO Team reported to the MOWG that it has enough propellant remaining to perform inclination maneuvers and other orbit maintenance maneuvers until 2016. After this time, CALIPSO may forego inclination adjust maneuvers and allow its node to drift with respect to Aqua's ascending node, but in such a way that it can continue data collection from the 705 km altitude. This in effect would constitute an exit from the A-Train. The exact course of action to be taken has not been decided, but whatever it is, it must be consistent with CALIPSO's EoM Plan.

Perhaps the satellite of greatest concern to the MOWG is CloudSat. This is for two reasons. The first is that CloudSat suffered a significant battery anomaly in April 2011 such that it no longer operates as it once did just after launch; rather, its operations have been modified forcing a new operational mode and operational constraints. In particular, CloudSat effectively hibernates during eclipse and recovers to functions nominally while in sunlight. Its new operational modes and constraints have invalidated the use of CloudSat's original EoM Plan as far as exiting the A-Train, and the anomaly made clear the need for CloudSat to stand ready at the first sign of trouble that could inhibit future maneuvering to initiate an A-Train exit.

The second reason has to do with CloudSat's current location in the A-Train. Just after launch, CloudSat was situated immediately in front of CALIPSO and behind Aqua. It is now located behind CALIPSO, Aqua, GCOM-W1, and after July 2014, OCO-2. This change in position was made as part of CloudSat's recovery from the battery anomaly and its return to A-Train operations in July 2012. Now when exiting the A-Train, CloudSat must safely navigate its way forward and below each of these satellites

The purpose of this paper is to discuss analyses done by the CloudSat team and considerations given to the

design of an effective, safe constellation exit strategy in spite of the new operating mode. Some of these topics, if not all of them, should be of interest to other missions considering the development of or modifications to their EoM Plan as lessons learned and things to watch out for when formulating an exit strategy.

## 2. CLOUDSAT'S ORIGINAL EOM PLAN

When CloudSat launched, it had an EoM Plan that included a maneuver strategy for exiting the A-Train. Per that plan, the A-Train exit strategy was to execute two equal magnitude maneuvers at opposite sides of the orbit to lower CloudSat's orbit and achieve a safe-exit-orbit situated below the remaining constellation satellites. It is from that point in its safe-exit-orbit that CloudSat would then proceed with further orbit-lowering maneuvers to eventually consume all of its remaining propellant. While the plan assumed the full range of CloudSat capabilities would be available for use at EoM, it was understood that certain parameters would not be the same as they were at launch. For example, propellant would be consumed during the course of the mission such that the amount left in the tank would depend on the number and size of maneuvers executed up to that point. Other parameters quantifying the spacecraft's health and well-being would also have changed simply due to normal wear and exposure to the space environment. Thus, the CloudSat team understood from the beginning that some modifications to the original plan would be required when the time came to exit the A-Train. That said, the basic plan was considered a blueprint to be redlined with modifications at the appropriate time.

The design of the A-Train exit maneuvers was based on a Hohmann Transfer from the A-Train orbit to a safe-exit-orbit situated below. To make this work, it was assumed that the spacecraft would be able to maneuver wherever it wanted on the orbit in daylight or eclipse. The maneuver magnitudes were matched at  $\approx 5$  m/sec with the first maneuver being executed at the ascending node and the second at the descending node. This is shown schematically in Fig. 2.

The first maneuver would reduce the semi-major axis (SMA) by  $\approx 9.4$  km and the perigee of the transfer ellipse 18.8 km below the A-Train.

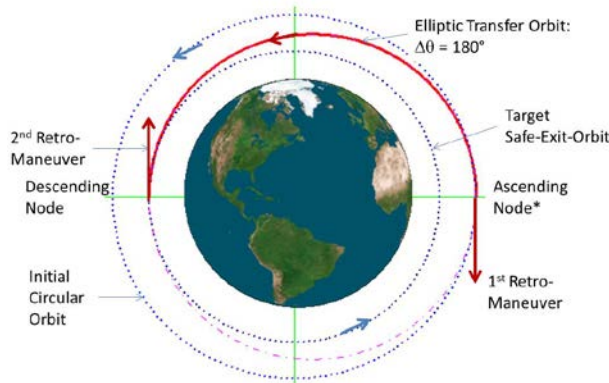


Figure 2. Hohmann Transfer Schematic for A-Train Exit

\* *CloudSat's sun-synchronous orbit has a Mean Local Time of the ascending node of  $\approx 13:45:45$  hrs; consequently, the ascending node is situated in sunlight and remains so.*

Again, the original CloudSat EoM Plan had the second exit maneuver set to occur  $1\frac{1}{2}$  to  $2\frac{1}{2}$  revolutions later, in eclipse at the transfer orbit's perigee.

As an interesting aside here, and a lesson learned is that we now know  $1\frac{1}{2}$  to  $2\frac{1}{2}$  revolutions ( $\sim 4$  hrs between maneuvers) is insufficient time to collect GPS tracking data, solve for the new orbit, transmit the ephemeris for the new orbit to Conjunction Assessment Risk Analysis (CARA) for screening, and then make a decision to execute the second maneuver based on an all-clear from CARA as far as the absence of conjunctions was concerned. Much more time is needed, and that fact was not recognized in the original EoM Plan. In the most recent CloudSat EoM Plan, the timing of the second exit burn is set to be after a much longer delay.

According to the original EoM Plan, the second exit maneuver would further reduce the SMA by about the same amount as the first maneuver,  $\approx 9.4$  km, but its principal purpose would be to decrease the apogee of the transfer ellipse sufficiently below the A-Train orbit, creating a new circular orbit approximately 19 km below the A-Train. With the final orbit well below the A-Train, the possibility of future conjunctions between CloudSat and A-Train satellites would be impossible without the use of further propulsion. CloudSat would

have achieved its safe-exit-orbit from which it could then begin a campaign of orbit lowering and decommissioning.

### 3. CLOUDSAT'S NEW OPERATIONAL MODE AND OPERATING CONSTRAINTS

After the battery anomaly in April 2011, there was a six-month recovery period before CloudSat was again operating in a semi-routine manner. To achieve this state, first, it was necessary to understand what had gone wrong during the anomaly. Second, the CloudSat team needed to formulate a new operating mode that would allow the spacecraft to function as much as possible like it did before the anomaly. The result was a new spacecraft-operating mode called Daylight Only Operations (DO-Op) (See Fig. 3). Analysis of the spacecraft's power system indicated that the battery was unable to support many of the normal loads through the eclipse period. This included fundamental hardware components such as the radar, taking cloud measurements, the propulsion subsystem, performing maneuvers, and the attitude control. [1,2]

In DO-Op mode, the spacecraft would shed power loads right before it entered the umbra such that only a handful of critical components were left powered-on. For example, the spacecraft's computer was kept alive with its memory and stored commands; the GPS navigation system also remained powered. Overall, however, the spacecraft was in a state of hibernation with many subsystems powered down. For example, there were no active attitude control functions. Instead, momentum stored as a momentum bias while the spacecraft operated in sunlight was transferred to the body axes when in eclipse causing the spacecraft to slowly spin in a preferred orientation. With this preprogrammed attitude, sunlight would fall on the solar panels restoring system power as soon as the spacecraft emerged from eclipse.

The most important of these restrictions and constraints to the constellation exit strategy was the fact that the spacecraft could not maneuver when in the Earth's shadow. All future maneuvers would have to be performed on the sunlit segment of the orbit.

**DO-Op: New nominal operating mode**  
**Point Standby: Part of layered response—used for maneuvers**

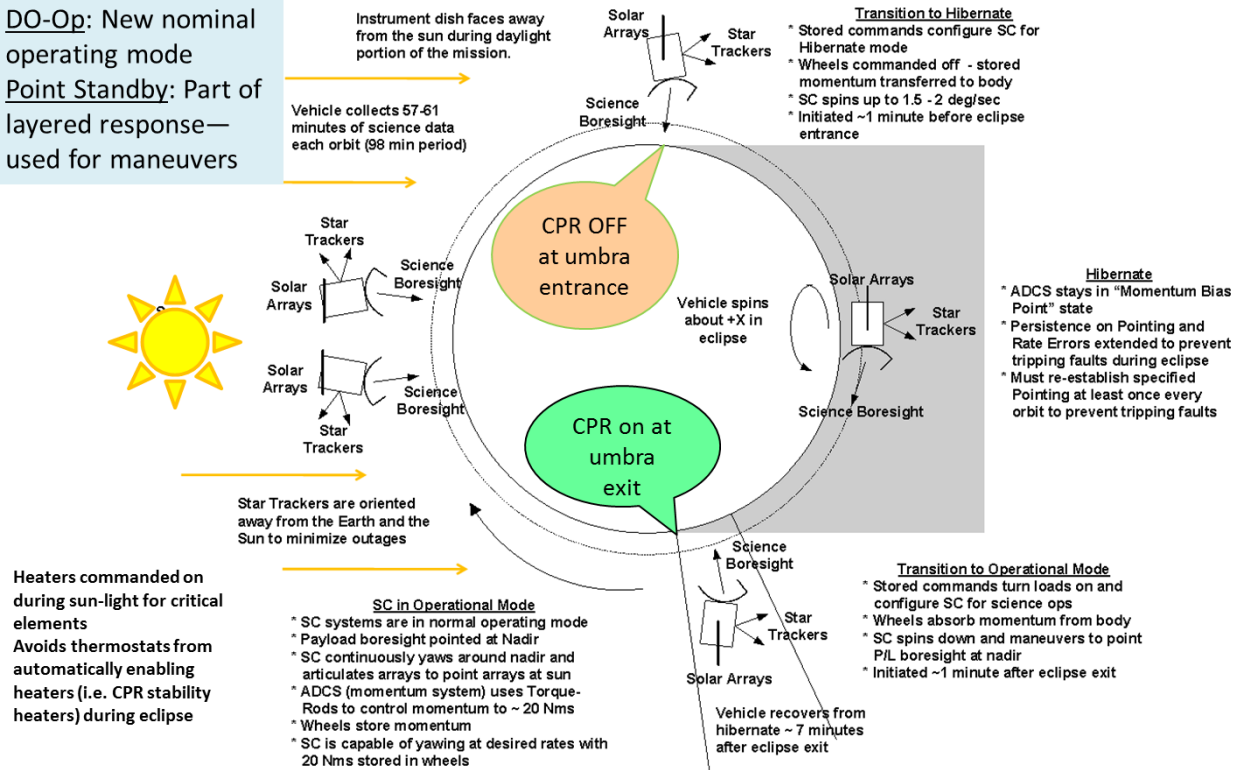


Figure 3. Do-Op Mode

#### 4. A-TRAIN ORBIT CHARACTERISTICS

Before analyzing constellation exit strategies, it is instructive to provide constellation configuration parameters, which quantify the dimensions of control boxes and the relative along-track spacings. Details of the A-Train's overall configuration and operating ground rules are contained in [4]. This reference includes a description of the A-Train in terms of placement of satellites along the orbit relative to Aqua and their allowed variation in location due to along-track movement relative to their designated location.

In particular, for this analysis we want to note that the satellites are spread along the orbit relative to one another but operate within their control boxes. The big picture view of the whole A-Train, including their

along-track positions with respect to each other, is shown in Fig. 1. However, for the purposes of this paper, only three satellites will be discussed. These are Aqua (AQ), CALIPSO (CP), and CloudSat (CS), as shown in Fig. 4. The same analysis results and conclusions derived from analyzing these adequately characterize the essential results; the inclusion of the remaining satellites, i.e., GCOM-W1, OCO-2, and Aura, would not alter the results.

In addition to along-track separation between boxes, measured in Equator Crossing Time Differences, it should also be noted that the A-Train satellites have their Mean Local Times of their ascending nodes offset from one another. Simply put, the orbits are close to but in fact not co-planar.

Tab. 1 below contains the relevant parameters

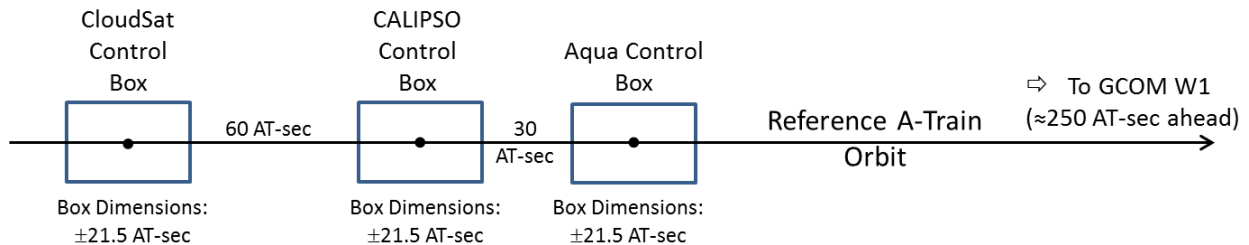


Figure 4. CloudSat, CALIPSO, and Aqua Constellation Control Boxes and Along-Track Spacings

Table 1. Aqua, CALIPSO, and CloudSat Geometric Orbit Parameters

Satellite	Equator Crossing Time $\Delta$ , sec	Along-Track Separation, sec	MLTAN, hrs	Angle of Asc. Node, $\Omega$ , deg	$\Delta\Omega$ , deg	Angle Between Orbit Planes, deg
AQ	0	0	13:35:00	23.75	—	—
AQ-CP	73	78.29	13:44:00	26.00	2.25	2.23
AQ-CS	176	182.32	13:45:45	26.44	2.68	2.66
CP-CS	103	104.03	—	—	0.44	0.43

specifying satellite positions with respect to Aqua and to each other. It also shows the Mean Local Time for each satellite and the respective MLT offset between satellites. These are the values used for these parameters in the subsequent analyses.

### 5. IMPULSIVE ANALYSIS OF EXIT MANEUVERS

We begin our study of the constellation exit problem by analyzing impulsive exit maneuvers. By impulsive we mean a delta-v imparted to a spacecraft instantaneously changing the orbital velocity, but not the position.

For this first examination of the problem, we shall simplify the analysis by assuming that all A-Train satellites move in circular, co-planar orbits. This circular orbit assumption is not a bad one given that the nominal eccentricity for A-Train satellites is on the order of 0.00118; with this small value the mean orbit is very nearly circular with the difference between semi-major and semi-minor axes being less than 5 m out of 7086 km. However, at the center, the circle is offset from the Earth's center by 8.4 km.

A convenient tool to use for analyzing this problem is the closed form solutions to Hill-Clohessy-Wiltshire (H-C-W) differential equations of relative motion. For those unfamiliar with the H-C-W equations, they describe the motion of a satellite on an elliptic, but near-circular, orbit with respect to another satellite on a circular orbit. D. Vallado gives an excellent discussion of the derivation of these equations, along with the derivation of their solutions, in [4]. For this analysis, we have programmed Vallado's solution into a software analysis tool capable of generating graphic solutions. Since we have for the moment restricted the effort to the problem of co-planar orbits, we concern ourselves with only the solutions for the radial and along-track (tangential) components of motion.

We begin by assuming that the reference circular orbit is the A-Train orbit. Since the A-Train satellites occupy an arc, which is approximately  $47^\circ$ , or 773 along-track seconds (Aura to GCOM W1) along the orbit, it is also convenient to flatten the circle into a straight-line coordinate axis. This is shown schematically in Figs. 1 and 4. The boxes shown are the respective control box for each satellite. These control boxes indicate to scale

the extent to which in-track motion for each satellite is permitted, per agreement between constellation members. A constellation satellite is therefore allowed to be anywhere along-track inside its respective box. If the motion of a satellite attempting to exit the A-Train should carry it into one of these boxes, this is a violation of the agreement and could cause a close conjunction between satellites.

Now we turn to CloudSat as an example and assume that it is going to make a 10 m/sec impulsive burn in order to initiate its exit from the A-Train. The impulse magnitude of 10 m/sec is an arbitrary number except that it is consistent with the size of impulse necessary to quickly leave the A-Train and lower CloudSat's orbit. Equally important, it displays all of the features of an initial exit maneuver of interest. Since all of the other A-Train satellites are moving along the circular orbit at the same angular velocity, their in-track positions remain contained inside their respective boxes and the boxes fixed with respect to CloudSat's maneuver point. CloudSat after the maneuver is now on a new slightly elliptical orbit and, more importantly, begins to move relative to these fixed boxes.

The initial exit maneuver is directed opposite to the orbital velocity. At first, CloudSat's motion is away from the point at which the maneuver occurred in the negative direction. However, because the orbital energy, SMA, and orbital period have all decreased, the motion quickly takes on a downward component relative to the reference orbit. In addition, CloudSat reaches maximum negative distance behind the maneuver point shortly after the maneuver ( $-4.5$  km at 684 sec) and then reverses the direction of its motion to be forward along-track. This motion reversal relative to the maneuver point can be seen by graphing the solution to the H-C-W equations, as shown in Fig. 5. Once the direction of motion reverses the relative velocity moves in the forward direction while the radial distance below the A-Train continues to increase, until the spacecraft reaches the perigee on its new elliptic orbit. After perigee, the radial separation between the spacecraft and the reference orbit decreases until apogee where the spacecraft is again at the reference orbit altitude. Fig. 6 shows the relative motion over one rev on an exploded scale picture, including the passages through perigee and the second apogee.

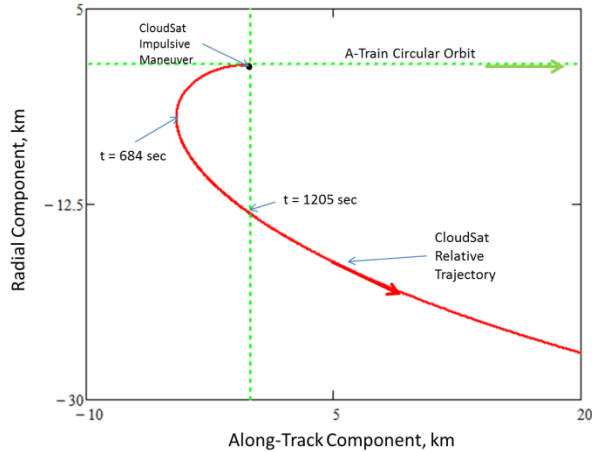


Figure 5. CloudSat Relative Trajectory to the A-Train Orbit after a 10 m/sec Impulsive Maneuver

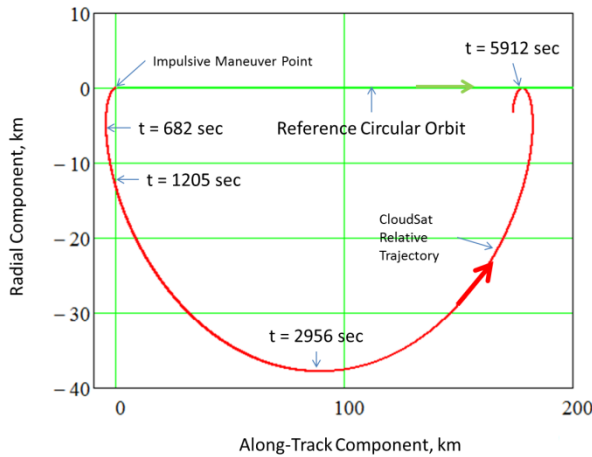


Figure 6. CloudSat Relative Trajectory to the A-Train Orbit after a 10 m/sec Impulsive Maneuver; Propagation through One Rev

When we propagate further in time, we observe that after each complete revolution on the new orbit it returns repeatedly to its apogee on the A-Train orbit.

Moreover, it reaches each new apogee at a point advanced 23.7 along-track seconds (178.1 km) forward along the orbit from the maneuver point. Thus, if we propagate forward for several revs, one or two of these apogee positions resulting from the 10 m/sec maneuver will fall inside of CALIPSO's control box. This is shown in Fig. 7 where CloudSat's trajectory relative to its maneuver position touches the circular orbit inside CALIPSO's box after 4 and 5 revs.

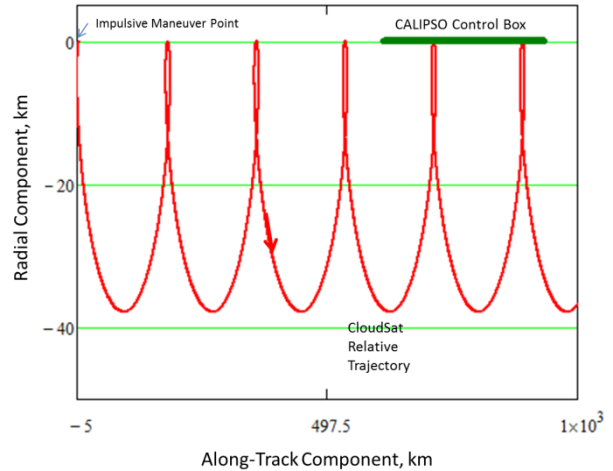


Figure 7. CloudSat Relative Trajectory to the A-Train Orbit after a 10 m/sec Impulsive Maneuver; Propagation through Five and a Half Revs

The message here, quite simply, is that the initial impulse to exit the A-Train results in the satellite making repeated returns to, or near to, the A-Train altitude at regularly spaced intervals. The along-track width of steps is dependent on the magnitude of the impulse. Furthermore, some of the returns to apogee occur inside the control boxes of constellation satellites forward of the exiting satellite. When these returns to apogee occur, the satellites involved need to be on alert for a possible close conjunction. In the example studied, CloudSat makes encroachments into the CALIPSO control box after 4 and 5 revs, while encroachments into Aqua's box do not occur until 7 and 8 revs. Because the control boxes for Aqua and CALIPSO are of the same dimensions, the 10 m/sec step size corresponds to only two encroachments into their respective boxes as CloudSat move along the orbit.

This analysis also implies a relatively short time scale after the exit maneuver until CloudSat makes encroachments. Given the violations of CALIPSO's box are just after 4, then 5, revs, this amounts to only 6.5 to 8.2 hrs after the maneuver. For Aqua, with its box centered 176 along-track sec further ahead on the orbit, CloudSat's encroachments would not occur until 16.4 to 18.0 hrs after the maneuver. This implies that these satellites should be well informed about CloudSat's plan for and timing of the constellation exit so they can be prepared to take actions should circumstances require.

In a worse case situation, where there is a spacecraft anomaly after the initial exit burn and the spacecraft is no longer able to maneuver, this analysis provides a quick means of estimating when the likelihood of close conjunctions will occur and how long until the exiting satellite has cleared the front of the constellation altogether.

## 6. FINITE BURN ANALYSIS

We have seen that an impulsive burn analysis is useful in establishing intuition and a general feel for what post-maneuver motion results when a sizeable exit maneuver is executed as the first step in leaving the A-Train. However, in the end it does not adequately represent what really goes on during a maneuver where thrusting lasts for more than 600 sec. This would be the case for maneuvers with magnitudes between 5 and 15 m/sec, or larger.

For a spacecraft like CloudSat, the larger magnitude maneuvers require a sizeable thrusting arc in order to achieve the desired delta-v. As an example, if we take thrust acceleration on the order of  $0.015 \text{ m/sec}^2$  (not untypical for a spacecraft well into its mission and approaching EoL), then the time spent thrusting is the order of 10 min or more (i.e.,  $>600 \text{ sec}$ ). With this maneuver magnitude, the spacecraft transfers through an orbit arc of  $36^\circ$ . A maneuver over this large arc does not qualify as impulsive; rather, it becomes important to use a finite burn analysis to account for gravity losses/gains and other effects.

For some missions, the use of finite burn modeling is routine and is the usual means by which a spacecraft's maneuver is simulated to establish the expected orbit change. After all, if one plans to use the analysis results as a means of determining the post-maneuver orbit ephemeris, a full-up simulation of the spacecraft, its propulsion system, and the thrusting along the arc is necessary to get a highly accurate estimate of the post-maneuver orbit. Also, with this accurate orbit ephemeris, ground station contact times and antenna look angles can be better determined and perhaps, more importantly, the orbit ephemeris will do a better job when input into a conjunction analysis for evaluation and in giving assurances that the maneuver does not place the spacecraft on a post-burn orbit with high risk of a close encounter with space debris.

On the other hand, and again using CloudSat as the example, all propulsive maneuvers executed during the mission were small in comparison to a constellation exit maneuver, i.e., less than 5 m/sec, and the impulsive approximation was quite adequate for estimating the post-burn orbit. In fact, for CloudSat the largest, single maneuver performed to date is 4.01 m/sec for an inclination change back in April 2012.

Because all CloudSat maneuvers required to date were relatively small, and because the impulsive approximation was adequate for simulating the change in the orbit, CloudSat used the impulsive maneuver approximation exclusively. Overall, it required less effort and provided results adequate to the mission's needs. However, the prospect of a 900 sec burn to exit

the A-Train is another matter and will demand that the CloudSat team use a finite burn analysis to evaluate with the desired accuracy the post-maneuver orbit.

Consequently, we shall now examine how the finite burn analysis differs from the impulsive maneuver analysis.

However, before proceeding, we need to mention a detail associated with the construction of an exit strategy using a finite burn analysis. When it comes time to exit the constellation, one has the choice of specifying a target delta-v for the first maneuver or specifying the burn duration and allowing the delta-v to vary accordingly as the propulsion system parameters vary with the changing propellant load. Both approaches have their merits and drawbacks, but for CloudSat the choice was to fix the burn time of the two exit maneuvers. When it comes to considering what to use, each mission must examine for itself the pros and cons of each approach and make its own choice.

With CloudSat choosing to use a fixed burn time for its constellation exit strategy, analysis indicates that the mission can continue to operate until thrust levels reach  $\approx 7$  newtons; at this thrust level the first exit maneuver magnitude is reduced from the initial 10 m/sec to approximately 8 m/sec, or slightly less. CloudSat will be at or near having just enough propellant left in the tank to perform its deorbit lowering maneuvers per its EoM Plan.

For the finite burn analysis discussed below, we have assumed CloudSat system parameters: mass, thrust, and mass-flow rate, consistent with the spacecraft's state back in April of 2012. Clearly, when it comes time for the real exit maneuver, the spacecraft's state at that time will dictate the system parameters to be used for the burn analysis. These parameters from April 2012 when evaluated in a finite thrust model yield a change equivalent to 10 m/sec delta-v from before and after the maneuver.

Also consistent with prior analyses, we assume the initial orbit to be circular. Therefore, when an impulsive retro maneuver occurs at a point on the initial orbit, that point becomes the apogee on the resulting elliptical orbit, since the position vector remains fixed before, during, and immediately after the maneuver. However, with a finite burn model, this is not so. The spacecraft position changes throughout the thrusting arc. Fig. 8 shows a simulation of a finite burn-thrusting arc for the spacecraft parameters discussed above indicating how the position of the spacecraft changes over the 900-sec burn as seen in a frame rotating with the circular orbit. The origin of this frame is centered on the start of the maneuver. The state vector at the point of burnout establishes the initial state for the post-burn elliptic

orbit. For comparison purposes, the 10 m/sec impulsive trajectory is also shown side-by-side with the finite burn trajectory in Figs. 8 and 9.

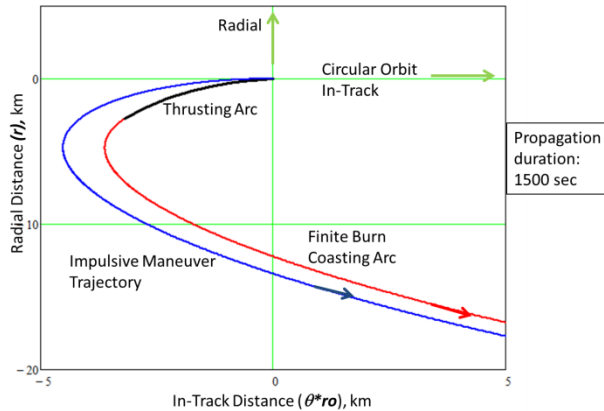


Figure 8. CloudSat Trajectories Relative to the A-Train Orbit, Comparing the Finite Burn with the Impulsive Maneuver

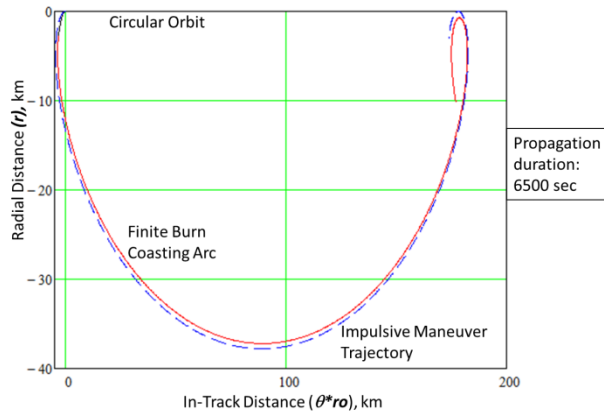


Figure 9. CloudSat Trajectories Relative to the A-Train Orbit, Comparing the Finite Burn with the Impulsive Maneuver: Propagation for One Rev

Just as before by propagating with the H-C-W model we can also see that the character of the trajectory after thrusting is very similar to the impulsive trajectory, as shown in Figs. 8 and 9.

So, what are the major differences between the results of the finite burn in comparison with the impulsive burn? Additionally, how are these differences computed? We know for the case of the impulsive burn that the position and post-maneuver velocity are used to compute a new SMA, eccentricity, and true anomaly. The radius and flight path angle remain unchanged. For the finite burn, we take the burnout radius, velocity, and flight path angle at the end of the thrusting arc and evaluate the same orbital parameters: SMA, eccentricity, and true anomaly. In order to determine comparable delta-vs we difference the SMAs before and after each burn; then using the linear partial derivatives for change in SMA as a function of change in velocity

magnitude, we obtain the effective burn delta-v. We can do the same for change in orbital period. Tab. 2 lists the post-maneuver orbital parameters for the two case studies of interest: the impulse burn vs. the finite burn.

Table 2. Comparison of Post-Burn Orbit Parameters for Impulsive Maneuver and Finite Burn

Post-Burn Orbital Parameter	Impulsive Burn	Finite Burn
Radius, km	7086.2308	7083.4959
Velocity, km/sec	7.5	7.492866
Flight Path Angle, deg	0.0	-0.0067628
Semi-Major Axis, km	7067.3970	7067.3349
Eccentricity	0.002665	0.002573
True Anomaly, deg	180	207.2338
Apogee radius, km	7086.2308	7085.5192
Perigee radius, km	7048.5632	7051.1524
Delta-SMA, km	-18.8338	-18.8959
Delta-V, m/sec	-9.9668	-9.9996
Delta-period, sec	-23.6673	-23.7453

From this comparison, we immediately note two important things: first, the position of the apogee is advanced for the finite burn case  $27.3^\circ$  to a point roughly midway through the thrusting arc. Second, we note that the apogee is lowered by approximately 712 m below the circular orbit radius. One of the effects of the finite burn is to provide head room relative to the original orbit, truly a fortuitous result.

## 7. INCLUDING EFFECTS OF NON-CO-PLANAR ORBITS

So far, we have assumed that the orbits of the A-Train satellites are co-planar. We have observed the conditions under which close conjunctions could occur and what to watch out for when designing an A-Train exit strategy. We will now add to this picture the effects of the orbit planes being slightly inclined with respect to one another.

Since Aqua is considered the anchor satellite for the A-Train, the Mean Local Time of the Ascending Node (MLTAN) for all other A-Train satellites is reckoned relative to Aqua's MLTAN. A satellite trailing Aqua in the A-Train but wanting to overfly the same identical ground track as Aqua would therefore have to shift its MLTAN appropriately to allow earth rotation by the same amount as the phase angle difference between it and Aqua. This tactic of this orbit design is common knowledge among mission designers and is used frequently to achieve a desired measurement congruency with other constellation satellites. The MLTAN differences, node angles, and angles between orbit planes are given in Tab. 3.

Table 3. Mean Local Time of Ascending Node and Angular Offsets for Aqua, CALIPSO, and CloudSat

Satellite	MLTAN, hrs	$\Omega$ wrt MSM, deg	$\Delta\Omega^1$ , deg	$\Delta\alpha^2$ , deg	$\mathcal{S}^3$ , deg
Aqua	13:35:00	23.75	—	—	—
CALIPSO	13:44:00	26.00	2.25	2.23	90.16
CloudSat	13:45:45	26.44	2.69	2.66	90.19
CS-CP	—	—	0.44	0.43	90.03

1. Angular arc from Mean Solar Meridian to the ascending node; for an unperturbed SSO this angle remains constant
2. Angle between orbit planes: CALIPSO to Aqua, CloudSat to Aqua, and CloudSat to CALIPSO
3. Angle measured along CloudSat orbit from the ascending node to the point of orbit plane intersection: CloudSat with Aqua; CloudSat with CALIPSO

The importance of this is that the trailing satellite's orbit is not co-planar with Aqua's orbit. In most cases, the offset is just a degree or two, but it is enough that two orbits will have ample cross-track separation between them except at the point where the two orbit planes intersect. For A-Train satellites, these points of intersection occur near the poles. At these points two satellites passing through simultaneously are close enough to give cause for concern of a collision occurring. These are the only two places on the orbit of either satellite where a close conjunction can happen.

For CloudSat exiting the A-Train, this is generally not a concern since the spacecraft must be making itself ready for umbra entrance or recovering for its latest passage through eclipse. In either case, CloudSat will not be maneuvering and therefore will always have a significant cross-track separation, i.e., several kilometers or more, when passing one of the satellites in front of it.

It is, however, important to note that this circumstance is satellite dependent and other constellation satellites may well have to concern themselves with conjunctions at the poles when designing their exit strategy, especial if the orbits are near co-planar and exit maneuvers are set to occur near the poles.

## 8. CLOUDSAT'S CURRENT PLAN FOR EXITING THE A-TRAIN

Taking advantage of the knowledge gained while studying the Hohmann Transfer exit strategy in the original CloudSat EoM Plan, CloudSat will use two orbit-lowering maneuvers separated along the orbit by the largest practical but achievable angle. The magnitude for these maneuvers will be as large as is deemed practical without incurring undue spacecraft risk and/or violating a constraint. The idea here being that CloudSat, in the worst case, wants to exit from the constellation as quickly and decisively as possible.

As noted before, DO-Op mode requires all of CloudSat's maneuvers to occur on the daylight portion of the orbit, i.e., somewhere between umbra exit and umbra entry. CloudSat's Sun-synchronous orbit experiences  $\approx 65 (\pm 1)$  minutes of sunlight per rev, regardless of the time of year. With the "in-the-sunlight" constraint on maneuvering, the new strategy will not be as effective or efficient in transferring CloudSat to a new orbit, as was the Hohmann Transfer where the angular separation between maneuvers was  $180^\circ$ . Nevertheless, the objective will be to achieve a safe-exit-orbit with just two maneuvers. The concept of a safe-exit-orbit is an orbit displaced sufficiently below the A-Train where there is no longer risk of close conjunctions with the remaining satellites. (The reader is referred to [6] for a more in depth discussion.) The safe-exit-orbit is a safe "waypoint" to be achieved below the constellation from which CloudSat can plan and initiate its campaign of additional orbit lowering maneuvers to consume eventually all remaining propellant, consistent with the EoM Plan.

In order to take best advantage of the 65 min of sunlight, CloudSat's first A-Train exit maneuver is positioned to occur over the southern hemisphere, beginning 686 sec after umbra exit. This elapsed time from umbra exit is required for the spacecraft to recover from its passage through eclipse and to orient the thrusters in an attitude appropriate for the orbit lower burn. The concept here, trying to emulate the Hohmann concept, is to execute the first exit maneuver as soon after umbra exit as is possible and then execute the second maneuver as close as possible to umbra entry. Additionally, fixing the maneuver start time this way ensures ample recovery time after the long thrusting arc for the spacecraft to reorient and prepare itself for umbra entry at the start of the next eclipse period.

Long before formulating the latest EoM Plan for CloudSat, constellation exit criteria were identified and limits for spacecraft parameters associated with exit criteria were defined. Limit violations trigger an immediate response from the ops team, including notification to the CloudSat Mission Director. The ops team, spacecraft team, and project management make a quick assessment whether to proceed with the constellation exit based on the exact nature of the limit violation and the health and well-being of the spacecraft. If circumstances do not warrant immediate constellation exit, the mission continues but in a heightened state of alert and readiness with the ops team on the watch for further out-of-limit conditions. If the assessment is to proceed with the EoM Plan, the team invokes A-Train exit procedures and prepares for exit maneuvers.

With the decision made to exit the A-Train, CloudSat must take a number of preparatory steps before maneuvering can begin. Telemetry retrieved from the spacecraft provides information about the spacecraft state (tank temperature, tank pressure, battery charge, etc.). From this, the expected thrust level, mass flow rate, and spacecraft mass are calculated. These parameters are all inputs to the finite burn analysis to determine an estimate for the post-maneuver orbit. The mission team uses an ephemeris for this new orbit internally to determine the timing of post-maneuver events and sends a copy of the ephemeris to CARA for a conjunction screening. Since the bulk of commands for the first maneuver are stored on the spacecraft, the only updates required to execute the maneuver are the commands authorizing execution and the Universal Time (UTC) for umbra exit on the selected rev. These are sent via uplink telemetry. The first exit maneuver has a magnitude of approximately 10 m/sec, or less, depending on the amount of propellant left.

In the meantime, the ops team determines telemetry transmit and retrieval opportunities after the maneuver so that emergency commands can be sent if necessary, but more likely, the retrieval of state-of-health telemetry can be planned. With the post-burn telemetry, the maneuver's effectiveness can be evaluated and any adjustments to the second exit maneuver determined. Assuming maneuver success is confirmed, preparations are begun for the second exit maneuver to be executed several days later.

This second exit burn is another orbit lower maneuver, but is much smaller in magnitude than the first maneuver. The burn duration is 180 seconds, corresponding to a delta-v of about 2.0 m/sec, or less. The reason for this smaller magnitude has to do with the desire to make the second exit burn as far removed as possible from the initial exit burn and still not incur a sun exposure violation for the radar instrument; thus, its location is as far north of the equator as possible within that constraint. Unfortunately, for orbit lower maneuvers north of the equator, direct sunlight falls onto the radar antenna and down the boresight. After studying the problem for all seasons, the CloudSat ops team decided to fix the mid-point of the maneuver 2925 sec after umbra exit ( $177^\circ$ ) and to limit the length of burn duration so as not to overheat the radar. The project dictated these actions to preserve the option to operate the radar after achieving the safe-exit-orbit. Owing to this maneuver's small size, impulsive maneuver analysis is justified and will be used for its evaluation.

Nominally, steps to prepare for the second exit maneuver are the same as for the first maneuver, but require more time to complete; therefore, the execution

is likely not to occur until about three to four days after the first maneuver.

In order to see why this strategy works for all seasons, we make a schematic of CloudSat's orbit relative to the orbit noon (Fig. 10). In the figure the positions of the two exit maneuvers are shown as red arcs adjacent to the orbit itself; the long arc is the first maneuver with 900 sec of burn duration while the short arc is for the second maneuver at 180 sec. Also shown is the position of the equator for two dates during the year (2012). These dates are not arbitrary but correspond to the sun making its greatest excursions north and south relative to the equator along the orbit in 2012. These excursions are due to the annual variation in the Sun's declination.

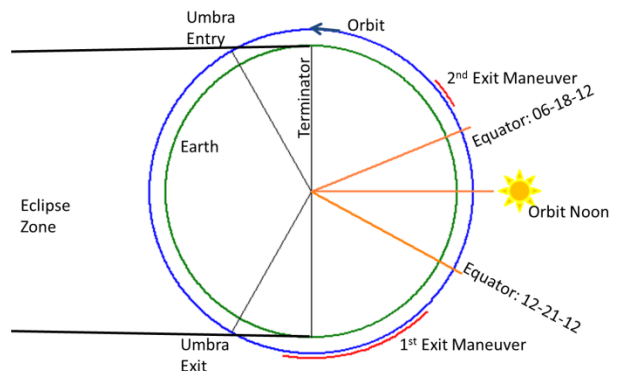


Figure 10. CloudSat Exit Maneuver Geometry with respect to the Sun

The effect of this is that the geographic positions (i.e., the subsatellite latitude) of the exit maneuvers swing north and south over the course of a year. Thus, the argument of latitude for the start of the first maneuver can be as much as  $100^\circ$  south of the equator along the orbit for maneuvers in December. Geographically, this corresponds to being at latitude of  $77^\circ$  south, before passing through the orbit's southernmost latitude,  $81.8^\circ$  south.

For maneuvers in June, near the summer solstice in the northern hemisphere, the argument of latitude for the start of the first burn will have moved north to be only  $47^\circ$  south of the equator (which has a geographic latitude of  $46^\circ$  south). In December, the argument of latitude for the second maneuver is  $36^\circ$  north. In June, the argument of latitude for the second maneuver is  $84^\circ$  with corresponding latitude of  $80^\circ$  north. Thus, we see that the exit maneuvers are always in the Sun year-round.

From the previous finite burn analysis, it was shown that a 10 m/sec maneuver lowers the SMA by  $\approx 19$  km and reduces the apogee altitude by  $\sim 700$  m. This is clearly one of the advantages of using a larger maneuver magnitude for exiting the constellation; the larger the maneuver, the greater the drop in apogee with that

maneuver. The large maneuver also repositions the argument of perigee. In particular, for the case where the first exit maneuver is done on 18 December, the argument of perigee is changed from 79.88° to 107.19°, post-maneuver. The second exit maneuver further changes the argument of perigee from 107.19° to 199.03°.

A summary of changes in orbital parameters for both exit maneuvers is contained in Tab. 4 below. Only the values for the argument of perigee are subject to change with calendar date.

Table 4. Comparison of Orbit Parameters Associated with the Two Planned A-Train Exit Maneuvers

Parameter	Initial Orbit <sup>1</sup>	1 <sup>st</sup> Elliptic Orbit <sup>2</sup>	2 <sup>nd</sup> Elliptic Orbit <sup>3</sup>
SMA	7086.23 km	7067.33 km	7063.57 km
Eccentricity	0.0	0.002573	0.002450
Arg of Perigee <sup>4</sup>	79.88°	107.19°	119.03°
Arg of Perigee <sup>5</sup>	132.70°	160.02°	171.86°
Apogee Radius	7086.23 km	7085.52 km	7080.91 km
Δ apogee	0.0 km	710 m	5.32 km
Perigee Radius	7086.23 km	7049.15 km	7046.23 km
Period	98.94 min	98.55 min	98.47 min
Synodic Period	undefined	17.36 days	14.39 days

1. Initial Orbit=parameters assumed for CloudSat's initial orbit while in A-Train
2. 1<sup>st</sup> Elliptic Orbit=parameters evaluated for CloudSat's orbit after the 1<sup>st</sup> exit maneuver (~10 m/sec); maneuver evaluated using finite burn analysis (900 sec)
3. 2<sup>nd</sup> Elliptic Orbit=parameters evaluated for CloudSat's orbit after the 2<sup>nd</sup> exit maneuver (~2 m/sec); maneuver evaluated using impulsive maneuver analysis
4. Argument of Perigee is a function of the calendar date of the maneuver; this data is for calendar date 21 December 2012, when the Orbit Noon is at an extreme position south of the equator
5. Argument of Perigee for this data is for calendar date 18 June 2012, when the Orbit Noon is at an extreme position north of the equator

Although the data in Tab. 4 is based on CloudSat's spacecraft parameters as they were in the spring of 2012, the analysis results provide strong evidence and confidence that the two-maneuver strategy will work and will place CloudSat in a safe-exit-orbit when the time comes to do so. However, the real orbit change resulting from the two maneuvers will depend on the spacecraft state (mass, tank pressure, etc.) when the decision is actually made to exit the constellation. The final orbit achieved may not be as robust as the one produced by the example analysis done here, but other analyses done by the CloudSat Project clearly suggest that the strategy will work and will successfully transfer CloudSat to a safe-exit-orbit when that time comes. After that, the CloudSat team will assess, based on the propellant remaining, the number and time for a

subsequent orbit lower campaign and the eventual passivation and decommissioning of the spacecraft at the mission's end.

#### ACKNOWLEDGEMENT:

The research described in this (publication or paper) was carried out at the Jet Propulsion Laboratory, California Institute of Technology, under a contract with the National Aeronautics and Space Administration.

#### REFERENCES:

1. Nayak, Michael, et al., *CloudSat Anomaly Recovery and Operational Lessons Learned*, SpaceOps 2012, June 2012, Stockholm, Sweden.
2. Gravseth, Ian, *CloudSat Recovery to Science Operations Following Battery Anomaly*, 35<sup>th</sup> Annual AAS Guidance and Control Conference, February 2013, Breckenridge, CO.
3. Manganis-Braun, Barbara, and Keenan, Donald, *CloudSat's A-Train Return: Solving the Orbital Dynamics Problem*. American Astronautical Society preprint: AAS 13-719, August 2013, Hilton Head, SC.
4. *Afternoon Constellation Operations Coordination Plan*, Earth Science Mission Operations Project, 428-10-08 Revision 1, GSFC/NASA, February 2011
5. Vallado, David, *Fundamentals of Astrodynamics and Applications* (Third Edition). Hawthorne, CA: Microcosm Press 2007.
6. Sweetser, Theodore, and Vincent, Mark, *The Eccentricity Behavior of Nearly Frozen Orbits*, American Astronautical Society pre-print, AAS 13-867, August 2013, Hilton Head, SC.